Chloride Binding in Cement Paste with Calcined Mg-Al-CO_3 LDH (CLDH) under Different Conditions

JIAN GENG[1,2*], CHONGGEN PAN[1,2], YU WANG[3], WEI CHEN[1,2] and YUEYUAN ZHU[1]

1 School of civil engineering and architecture, NingboTech University, China

2 Ningbo Research Institute, Zhejiang University, China

3 School of Science, Engineering & Environment, University of Salford, UK

* Correspondence: gengjian@nit.net.cn

Abstract: The chloride binding capacity of cement paste with Mg-Al CLDH, obtained through calcining a commercial LDH, is investigated under different chloride concentration, environmental temperature, and concrete pore solution alkalinity conditions. The transformation mechanism of Mg-Al CLDH to Mg-Al-Cl LDH is mainly explored by means of X-ray diffraction (XRD) , Fourier-transform infrared spectroscopy (FT-IR) and Differential thermogravimetric analysis (DTG). There appears to be a threshold chloride concentration of 1.0 mol/L for Mg-Al CLDH (6% incorporation) effectively enhancing the chloride binding capacity of cement paste. Both lowering and raising (> 38 °C) the environmental temperature is disadvantage to the transformation of Mg-Al CLDH to Mg-Al-Cl LDH in cement paste，and the amount of bound chloride at different curing temperatures follows as 38 °C > 50 °C ≈ 20 °C > 3 °C. Higher pore solution alkalinity is also adverse to both of the formation of Friedel's salt and the rehydration of CLDH. With increasing pH from 12.5 to 13.5, the improvement of Mg-Al CLDH on the chloride binding capacity of cement paste became weaker. Mg-Al CLDH improves the chloride binding capacity of cement paste is not only related to the excellent anions exchanging ability of it , but also related to the promotion of Friedel's salt formation of it.

Keywords: Calcined layered double hydroxide; Chloride binding; Cement paste; Temperature; Alkalinity

Highlights:

(1) The transformation mechanism of Mg-Al CLDH to Mg-Al-Cl LDH in cement paste under different conditions is analyzed by using XRD, DTG and FT-IR;

(2) The optimum temperature range for the formation of Mg-Al-Cl LDH in cement paste is from 20 to 38 °C;

(3) Higher pore solution alkalinity is adverse to both of the formation of Friedel's salt and the rehydration of CLDH;

(4) The use of Mg-Al CLDH can promote the formation of Friedel's salt in cement paste.

1. Introduction

The corrosion of steel rebars used in concrete is expedited when there is chloride contamination. Research has shown that only free chloride ions cause the corrosion of steel rebars. However, under these conditions, chloride ions content, the free and bound chloride in the concrete, can have a direct influence on the corrosion of steel rebars. Therefore, improving the chloride binding capacity of cement-based materials has been regarded as an effective method to reduce the corrosion risk of steel rebars used in concrete.

The addition of supplementary cementitious materials (SCMs), such as fly ash (FA), ground granulated blasted-furnace slag (GGBS) and metakaolin, will improve the chloride binding capacity of concrete[1,2]. However, the effective chloride binding capacity is limited by the amount of reactive alumina ($Al_2O_3^{r-}$), which can react with free chloride to form Friedel's salt (FS) in these SCMs[3,4].

In recent years, layered double hydroxides (LDHs) have been used to improve concrete durability[5-8]. LDHs can be expressed in a general formula $[M_{1-x}^{2+}M_x^{3+}(OH)_2]^{x+} \cdot A_{x/2}^{n-} \cdot mH_2O$, where M^{2+} and M^{3+} represent divalent and trivalent metal ions, respectively (i.e. Mg^{2+}, Al^{3+}, etc.), while A^{n-} represents an interlayer anion, such as CO_3^{2-}, SO_4^{2-}, OH^-, F^-, Cl^- or NO_3^-, and x is the ratio $M^{3+}/(M^{3+}+M^{2+})$ [9]. The structures of LDHs mean they have an excellent potential for anion exchange. In addition, LDHs also demonstrate another important character of material memory, which means that the crystal phases of the LDHs will decompose in the temperature range of 500-600 °C to form a new crystal structure called calcined LDHs (CLDHs or LDOs). However, CLDHs can rehydrate to LDHs when appropriate anions enter into their layered crystal structure through aqueous solution. Taking the LDH of Mg-Al-CO_3 as an example, its thermal decomposition and rehyration process can be illustrated through the following reactions [10].

$$Mg_{1-x}Al_x(OH)_2(CO_3)_{\frac{x}{2}} \cdot mH_2O \rightarrow Mg_{1-x}Al_xO_{\left(1+\frac{x}{2}\right)} + \frac{x}{2}CO_2 + (m+1)H_2O \quad (1)$$

$$Mg_{1-x}Al_xO_{\left(1+\frac{x}{2}\right)} + \left(\frac{x}{n}\right)A^{n-} + \left(m+1+\frac{x}{2}\right)H_2O \rightarrow Mg_{1-x}Al_x(OH)_2(A^{n-})_{\frac{x}{n}} \cdot mH_2O + xOH^- \quad (2)$$

This example shows that the rehydration processes of CLDHs not only involves the adsorption of chloride ions, but also the release of hydroxide ions, which benefits for increasing the corrosion resistance of steel rebars. Attempts to improve reinforced concrete durability by using LDHs and CLDHs as functional materials in order to adsorb chloride ions has also been investigated. Yoon *et al.* modeled the chloride adsorption of rhydrated Mg-Al CLDH through a cement matrix and proposed that rehydrated Mg-Al CLDH has an extraordinary potential in preventing the deterioration induced by chloride[11]. Chen *et al.* also found the chloride binding capacity of rehydrated Mg-Al CLDH was far better than cement paste and pure fly ash, and Mg-Al CLDH could improve the durability of Ultra-High performance concrete in chloride environment[12]. Besides, the chloride binding capacities of other types of LDHs in cement-based materials also have been investigated. Chen *et al.*have demonstrated that the Ca-Al-NO_3 LDH can immobilize chloride in hardened cement pastes, but only under low sulfate and carbonate environments, because the ion exchange process between NO_3^- and Cl^- could be interrupted by the presence of SO_4^{2-} or CO_3^{2-}[13]. Yang and Fischer *et al.* synthesized two modified hydrotalcites (MHT), using nitrate and aminobenzonate (pAB) anions (i.e., Ca-Al-NO_3 MHT and Ca-Al-pAB MHT)[14]. These modified hydrotalcites were used in a simulated concrete pore solution with a rich chloride content and subsequently a reduction of the free

chloride concentration was observed. In general, rehydrated CLDHs have shown excellent chloride binding capacities compared with LDHs in cement pastes.

It should be mentioned that environment temperature and solution alkalinity, also have important effects on chloride adsorption of CLDHs, as well as the intrinsic attributes of them. Lv *et al.* investigated the use of CLDHs for environmental cleanup and remediation of contaminated water[15]. The Mg-Al CLDH was chosen for its chloride removing capacity and the effects from the amount of chloride and the temperature were studied. A study by Zhang *et al.* found that a temperature of 30 °C and pH between 5 to 11 were optimum for the Mg-Al-Fe CLDH to absorb chloride from waste water[16]. In summary, the changes of temperature and pH on chloride adsorption of CLDHs are significant. But, seldom similar works have been done based on cement based materials. The mechanism of the chloride binding process and characterization in cement pastes, especially for the transformation of CLDH to LDH considering the changes of environmental temperature and pore solution alkalinity, is currently incomplete and limited.

Therefore, the chloride binding capacity of cement paste with Mg-Al CLDH, obtained through calcining a commercial LDH, was investigated under different conditions. Based on this, this study focused on the chloride adsorption process of rehydrated Mg-Al CLDH, and the transformation of CLDH to LDH due to the changes of chloride concentration, environmental temperature, and concrete pore solution alkalinity, to further understand the effect mechanism of CLDH on the chloride binding capacity of cement paste.

2. Experiment

2.1. Materials

The cement used in this study is Portland Cement P.O. 42.5. The mixing water used was deionized water. Mg-Al CLDH was obtained through thermally treating commercial Mg-Al-CO_3 LDH (supplied by Allison (Beijing) Technology Co. LTD, $Mg_6Al_2(OH)_{16}(CO_3)(H_2O)_4$) at 500 °C for 5 h with a heating rate of 4 °C/min. Then, Mg-Al CLDH was ground into a fine powder and sieved using a mesh with a 0.16 mm aperture size. The sieved powder was then stored in a sealed container to prevent carbonation before use. The chemical compositions of the cement and Mg-Al-CO_3 LDH detected by X-Ray Fluorescence (XRF) technology are listed in Table 1.

2.2. Methods

Two different cement paste mixes were tested in this study, which are listed in Table 2. All paste samples were cast into 40 mm × 40 mm × 40 mm sizes and made using a fixed water to cement ratio of 0.42. After casting, all samples were at first cured in molds under 20 ± 2 °C and 95 % RH for 1 day. Following the first day, the samples were demolded and continuously kept under the same condition for another 27 days. The samples were then broken into small blocks on the order of 0.315-2.5 mm and stored in a desiccator containing silica gel and soda lime to protect from carbonation.

Chloride binding tests were conducted using the equilibration method. Each test used 20 g of the dried small cement paste blocks that were placed inside a 200 mL glass bottle. Then, 100 mL of a mixture of sodium chloride solution and saturated calcium hydroxide solution (SCHS) was added. Three tests were conducted for each mix. First, small sample blocks of the cement paste were immersed in SCHS with added chloride concentrations of 0.05, 0.25, 0.5, 1.0, 2.0 and 2.5 M, respectively. The samples prepared in this way were denoted as group A. This test was conducted at 20 °C to obtain chloride binding isotherms (CBI). Next, small sample blocks of the

cement paste were immersed in the SCHS with 0.5 M Cl^- and were then held at four different temperatures of 3, 20, 38 and 50 °C. The samples prepared in this way are denoted as group B. Lastly, the pH of the SCHS was changed with the addition of 0.1 M NaOH solution to 12.5, 13.0 and 13.5, while the chloride content was kept at 0.5 M and temperature was controlled at 20 °C. The samples prepared in this way are denoted as group C. The total immersion time for all the tests was 60 days, in which the glass bottles were periodically shaken to maintain solution homogeneity. Table 3 lists the detailed experimental conditions for each group of samples, and the total number of samples of very mix is 19.

After the chloride binding tests were performed, the small sample blocks were dried at 50 ℃ for 24h, ground into a fine powder, and then sieved using a 0.16 mm mesh. All the passed particles were stored in a desiccator containing silica gel and soda lime to minimize carbonation before they were used for material characterization analyses.

Under equilibrium, the concentration of free chloride (C_e, mol/L) in solution was measured using the traditional leaching method according to the Test Code for Hydraulic Concrete (SL352-2006) standard. The bound chloride content (C_b, mg/g) in hardened cement paste was calculated using the following equation:

$$C_b = \frac{35.453 \times (C_i - C_e) \times V_{SCHS}}{m_{total}} \quad (3)$$

where C_i is the initial total chloride ion content in the SCHS (mol/L), V_{SCHS} is the volume of SCHS (mL), m_{total} is the mass of small sample blocks (g), and 35.453 is the molar mass of chloride ions (g/mol).

X-ray diffraction (XRD) analysis was carried out using the D8 Advance instrument of Bruker AXS with a Cu Kα radiation generated with 40 kV and 30 mA. The diffraction patterns were collected in the range of 5 – 60 ° (2θ) scale, with a step size of 0.02 °/s. Fourier-transform infrared spectroscopy (FT-IR) was performed on the samples using a Nicolet Nexus 470 spectrometer with the KBr pellet technique in the range of 400 – 4000 cm^{-1}. Differential thermogravimetric analysis (DTG) were carried out using a Netzsch TG-209F1 thermal analyzer, using a heating rate of 20 °C/min at the range of 25 – 1000 °C in air.

3. Results and discussion

3.1. Chloride binding isotherms (CBIs)

Fig.1 depicts the chloride binding isotherms of C0 (A) and CLDH6 (B) under standard curing conditions (20 ± 2 °C and 95 % RH). The linear, Langmuir, Freundlich and BET models can be used to express the relationship between the free and bound chloride ions in cement paste[17]. Among these models, the Langmuir and Freundlich models are the most widely discussed, and they are represented by Eqs (4) and (5), respectively:

$$C_b = \frac{QbC_e}{(1 + bC_e)} \quad (4)$$

$$C_b = K_F C_e^n \quad (5)$$

where Q and b are the Langmuir constants, K_F and n are the Freundlich constants, and C_e is the equilibrium concentration of chloride ions in a SCHS (mol/L).

Fig.1(A) shows the CBIs for C0, which does not have any Mg-Al CLDH. Using Eqs. (4) and (5) to fit the experimental data, the Freundlich model results in a better fit than the Langmuir model. This result is consistent with other reports[1, 18, 19]. For C0, the best-fit Langmuir parameters are Q=89.3 $mg \cdot g^{1}$ and b=0.19 $ml \cdot L^{-1}$, and the best-fit Freundlich parameters are K_F=14.14 and n=0.79.The CBI for CLDH6, which has Mg-Al CLDH, is shown in Fig.1(B). Compared to the fitting of C0, the fitting of CLDH6 is very similar for both models. This result is different than Yoon *et al.* who concluded that the CBI of cement paste with CLDH was better described by the Langmuir model[11]. In this case, for CLDH6, the best-fit Langmuir parameters are Q=152.3 $mg \cdot g^{1}$ and b=0.42 $ml \cdot L^{-1}$ (which are very close to the fitting result of Yoon *et al.*), and the best-fit Freundlich parameters are K_F=17.28 and n=0.83.

Comparing the experimental data from C0 and CLDH6 at the same chloride concentration and Q values, CLDH6 has a higher bound chloride content (C_b) than C0. This confirms that adding Mg-Al CLDH significantly improved the chloride binding capacity of cement paste. It also should be noted that this improvement is closely related to the free chloride concentration in the cement paste. When the free chloride concentration is lower than 1.0 mol/L, the C_b values of C0 and CLDH6 are very similar. This suggests that the improvement in the chloride binding capacity of cement paste with Mg-Al CLDH appears to have a threshold concentration and the effect became more prominent as the chloride concentration increases.

3.2. The effect of environmental temperature

Environmental temperature is an important factor which can affect the chloride binding capacity of cement paste. Four temperatures were chosen to study this effect, namely 3, 20, 38, and 50 °C. Fig.2 shows the results of the two mix pastes, C0 and CLDH6, exposed to different chloride concentrations at different environmental temperatures. It can be seen that all samples exhibit increased chloride binding capacity with temperature until 38 °C, similar to what was observed by Lv *et al.*[15]. The amount of bound chloride at different curing temperatures follows as 38 °C > 50 °C ≈20 °C > 3 °C. However, compared with C0, the effect of temperature on the chloride binding of CLDH6 is more obvious, especially as the chloride concentration reaches to 1.0 M. This indicates that the use of Mg-Al CLDH leads to chloride binding capacity of cement paste becomes more susceptible to the change of environmental temperature. Fig.2 also shows that the improvement in the chloride binding capacity of the Mg-Al CLDH samples is more significant with larger chloride concentrations and higher environmental temperatures. This result is consistent with the results presented in section 3.1.

3.3. The effect of pore solution alkalinity

The optimum alkalinity of aqueous solution for the adsorption of CLDHs on anions is between pH 3.0 to 10.0, which is far lower than the alkalinity of pore solution (pH 11.0~13.5) in Portland cement pasts (no neutralization reaction). This means that the chloride adsorption capacity of Mg-Al CLDH in cement paste will be weakened. Nevertheless, from Fig.3, it can be

seen that the sample with Mg-Al CLDH has higher bound chloride content compared with the sample without Mg-Al CLDH, demonstrating that the use of Mg-Al CLDH can still effectively improve the chloride binding capacity of cement paste even at high alkalinity condition.

The result from Fig.3 also shows that the amount of bound chloride decreases with the pH of the pore solution increasing. When the pH is greater than 13.0, the chloride binding capacity deteriorated very fast, demonstrating that high alkalinity condition is adverse to chloride binding in cement paste with and without Mg-Al CLDH, and the enhancement of the chloride binding capacity by Mg-Al CLDH is also weakened under high alkalinity conditions (> 13.0). Otherwise, according to the data shown in Fig.3, when pH increases from 12.5 to 13.0, the drop rates of Cb for C0 and CLDH6 are 70.3% and 72.3%, respectively, indicating that the negative effect of high pH on chloride binding of sample CLDH6 is slightly serious compared with sample C0. Combining with the results from Section 3.2 and 3.3, it can be concluded that the use of Mg-Al CLDH not only improve the chloride binding capacity of cement paste, but also make it is susceptible to the change of temperature (from 3 °C to 50 °C) and pore solution alkalinity (pH value from 12.5 to 13.5).

3.4. Micro characteristic analyses of cement paste with and without Mg-Al CLDH

3.4.1. X-ray diffraction (XRD)

In XRD pattern, the characteristic peaks of Friedel's salt and Mg-Al-Cl LDH are very similar. For example, the strongest peak of two crystal phases in 2θ degrees, are 11.377° for the Friedel's salt (002) plane (PDF 31-0245, d=0.777 nm) and 11.248° for the Mg-Al-Cl LDH (003) plane (d=0.789 nm)[20]. Therefore, it is difficult to accurately distinguish between Friedel's salt and Mg-Al-Cl-LDH in full XRD pattern (2θ is from 5°-60°). To better understand the relationship between the formation of Mg-Al-Cl LDH and chloride concentration in cement paste, the XRD peaks of C0 and CLDH6 in the range of 2θ = 10° - 12° are depicted in Fig.4. From it, the characteristic peaks of C0 and CLDH6 mainly appear in the range of 2θ = 11.0° - 11.5°. As for CLDH6 samples, the characteristic peak of Mg-Al Cl LDH (d_{003} at 2θ =11.22° is 7.860), except for CLDH6-0.05M, can be clearly detected, confirming the transformation of Mg-Al CLDH to Mg-Al-Cl CLDH, and the change in intensity is directly proportional to the chloride concentration increasing from 0.5M to 1.0M. The absence of characteristic peak of Mg-Al Cl LDH in CLDH6-0.05M, can be contributed to the lower initial chloride concentration limiting the formation of Mg-Al Cl LDH. Besides, it can be found that the intensity of the peak of Friedel's salt from CLDH6 is higher than from C0, suggesting there is more Friedel's salt in CLDH6.

Fig.5 depicts the XRD patterns of C0-0.5M and CLDH-0.5M at different environmental temperatures. The effect of the environmental temperature on the formation of Friedel's salt is clear, and it can be separated into three stages. First, when the environmental temperature is 3 °C, the intensity of the Friedel's salt peak in the C0 sample is very weak, suggesting little Friedel's salt is present. Second, when the temperature is raised from 3 to 38 °C, there is a noted increase in the intensity of the Friedel's salt peak for both C0. Third, when the temperature increases further from 38 to 50 °C, the intensity of Friedel's salt peak in C0 decreases slightly.

As for samples CLDH6, though the temperature is only 3 °C, the peak of Mg-Al Cl LDH can be clearly detected in Fig.5(B), indicating the transformation of Mg-Al CLDH to Mg-Al Cl LDH under lower temperature condition which is different from the formation of Friedel's salt as shown in Fig.5 (A). From Fig.5 (B), it can be seen that the intensity of Mg-Al-Cl LDH peak

become stronger as the temperature elevating from 3 °C to 20 °C. However, when the temperature elevates from 20 to 50 °C, there was no an obvious increase of the Mg-Al-Cl LDH peak intensity, suggesting that the formation of Mg-Al CLDH is hampered at the higher temperature. As the same time, the peak of Friedel's salt in samples CLDH6-38 °C and CLDH6-50 °C becomes main peak comparing with samples CLDH6-3 °C and CLDH6-20 °C. This hampering of Mg-Al-Cl LDH formation is undoubtedly disadvantage to chloride binding in cement paste and is also the main reason for the decrease in bound chloride content seen in CLDH6-0.5M at 50 °C, as shown in Fig.2. It is concluded that the optimum temperature range for the formation of Mg-Al-Cl LDH in cement paste is from 3 to 38 °C, according to XRD results.

Fig.6 depicts that the XRD patterns of C0-0.5M and CLDH6-0.5M under different pore solution alkalinity conditions. Since higher pore solution alkalinity can hamper the formation of Friedel's salt, there is a significant decrease in the intensity of the Friedel's salt peak as the pH value increased in both C0 and CLDH6. This decrease in the Friedel's salt concentration leads to a decrease in the bound chloride content, as shown in Fig.3. It is noted that the intensity of the Friedel's salt peak in CLDH6 was still far higher than in C0, even when the pH was 13.5. Combined with the results presented in Fig.6 (B), the use of Mg-Al-Cl CLDH in cement paste can promote the formation of Friedel's salt, even at very high pH. According to Fig.6 (B), high alkalinity has negative effect on the formation of Mg-Al-Cl LDH in the cement paste. When the pH increases to 13.5, the intensity of the characteristic peak from Mg-Al-Cl LDH obviously becomes weak, which undoubtedly reduces the chloride binding capacity of the cement paste.

Otherwise, by comparing the change in the intensity of Friedel's salt diffraction peak from C0 and CLDH6 as shown in Fig.4, 5 and 6, it can be found that the latter has stronger peak, indicating there is more Friedel's salt in samples with Mg-Al CLDH. Therefore, it can be concluded that the use of CLDH in cement pastes is good for the formation of Friedel's salt in cement paste.

3.4.2. Differential thermogravimetry (DTG)

In order to further clarify the effects of chloride concentration, environmental temperature, and pore solution alkalinity on the formation of Mg-Al-Cl LDH in cement paste, the samples were analyzed with differential thermogravimetric analysis (DTG).

The DTG curves of C0-0.5M, CLDH6-0.5M, and CLDH6-1.0M, at 20 °C and pH 12.5, are shown in Fig.7. There are a few notable endothermic peaks present in the DTG curves. The peak near 100 °C is attributed to the dehydration of the C-S-H gel and ettringite (AFt), which are difficult to distinguish because they have similar dehydration temperatures, from 85 to 130 °C. The peaks near 160, 350, 450, and 700 °C are attributed to the dehydration of hydrated calcium aluminates (AFm), Friedel's salt, and portlandite, as well as the decomposition of calcite[19]. The peak near 350 °C for samples with CLDH, should be attributed to the dehydration of Mg-Al-Cl LDH and Friedel's salt[21]. There is also a shoulder peak near 210 °C only in the samples with Mg-Al CLDH, owning to the decomposition of OH- in layered structure of Mg-Al-Cl LDH[20]. It should be noted that the intensity of the peak near 350 °C in the cement sample with Mg-Al CLDH is higher than the corresponding peak in sample without Mg-Al CLDH, which is consistent with the XRD results shown in Fig.4.

The intensity of the AFm endothermic peak in CLDH6 is greater than in C0, where AFm is the general name for hydrated calcium aluminate phases. AFms are similar to LDHs and have a representative formula of $[Ca_2(Al,Fe)(OH)_6]\cdot X\cdot mH_2O$, where the brackets indicate the composition of a positively charged layer unit and X is the anion used to balance the excess positive charge[22]. In the domain of cement chemistry, X usually is SO_4^{2-}, CO_3^{2-} , Cl^-, or OH^-, while the corresponding AFm phases are known as monosulfoaluminate ($3CaO\cdot Al_2O_3\cdot CaSO_4\cdot 12H_2O$,$SO_4^{2-}$-AFm), monocarbonaluminate ($3CaO\cdot Al_2O_3\cdot CaCO_3\cdot 11H_2O$, CO_3^{2-}-AFm), Friedel's salt ($3CaO\cdot Al_2O_3\cdot CaCl_2\cdot 10H_2O$, Cl^--AFm) and Hydroxy-AFm ($3CaO\cdot Al_2O_3\cdot Ca(OH)_2\cdot XH_2O$, OH-AFm, which is unstable and decomposes to hydrogarnet (C_3AH_6) and portlandite)[23]. There are two endothermic peaks related to the dehydration of AFm phases in the DTG curves of C0 and CLDH6. The peak near 350 °C belongs to Cl^--AFm and references attribute the peak near 160 °C to SO_4^{2-}-AFm and/or CO_3^{2-}−AFm[24,25]. Though both SO_4^{2-}-AFm and CO_3^{2-}-AFm belong to the AFm family, the crystallinity of SO_4^{2-}-AFm is lower than that of CO_3^{2-}-AFm. This means that the latter would be more easily detected by XRD, if it exists in the cement paste. Since, there are no obvious diffraction peaks from CO_3^{2-}-AFm in the XRD patterns presented in Fig.7, this suggests that the endothermic peak near 160 °C is mainly due to the dehydration of SO_4^{2-}-AFm. When sample is exposed to high chloride conditions, SO_4^{2-}-AFm played an important role in the formation process of Friedel's salt because it could undergo anion exchange between the SO_4^{2-} in monosulfoaluminate and the Cl^- present in pore solution. When there is a higher concentration of SO_4^{2-}-AFm in the cement, there is a greater chance that Friedel's salt is formed, which is the reason that more Friedel's salt is observed in the analysis of CLDH6 samples as XRD shown.

The DTG curves of CLDH6-0.5M cured at 3, 20, and 50 °C with same pore solution alkalinity are shown in Fig.8. Due to the lower hydration activity of cement at low curing temperatures, the endothermic peak intensity of the C-S-H gel and AFt in CLDH6-3°C is far lower than in CLDH6-20°C and CLDH6-50°C. The most significant difference among the three samples is the absence of the Mg-Al-Cl LDH peak in CLDH6-3°C and CLDH6-50°C, which also proves that curing temperature is a key factor in determining the transformation of CLDH to Mg-Al-Cl LDH in cement paste. The results from XRD as shown in Fig.5 has proven the existence of Mg-Al-Cl LDH in above two samples, but the absence of it in the DTG analysis results indicates that the amount of Mg-Al-Cl LDH is little, demonstrating that both lowering and raising the environmental temperature is disadvantage to the transformation of Mg-Al CLDH to Mg-Al-Cl LDH in cement paste, and the optimum temperature range for it is from 20 to 38 °C.

Fig.9 depicts the DTG curves of CLDH6-0.5M with different pore solution alkalinities at 20 °C. The endothermic peaks of AFm, Mg-Al-Cl LDH, and Friedel's salt can all be easily detected in both CLDH6-12.5pH and CLDH6-13.0pH. There is no obvious difference between the DTG curves of the two samples as the pH increases from 12.5 to 13.0, suggesting that this change of alkalinity does not significantly affect the formation of AFm, Mg-Al-Cl LDH, or Friedel's salt. This also may be the main reason why there was only a slight decrease in the bound chloride content between CLDH6-13.0pH and CLDH6-12.5pH. Increasing the pH to 13.5, leads to significant changes, especially from 100 to 400 °C, in the DTG curve of CLDH6-13.5pH compared to CLDH6-12.5pH and CLDH6-13.0pH. The most significant change is the disappearance of the endothermic peaks of AFm and Mg-Al-Cl LDH, which results in the drastic decrease in the bound chloride content of CLDH6-13.5pH, shown in Fig.3.

343 3.4.3. Fourier transform infrared (FT-IR)

344 The FT-IR spectra for C0 and CLDH6 with different initial chloride concentrations at 20 °C
345 and pH 12.5 are shown in Fig.10. The band near 3642 cm^{-1} is due to the stretching vibration of
346 -OH in $Ca(OH)_2$. The changes in the bands near 3440 and 1637 cm^{-1}, are attributed the stretching
347 vibration of -OH in structural water found in the hydration products and the bending vibration
348 of -OH in the interlayer water present in hydration products, respectively. The intensities of
349 these two bands (3440 and 1637 cm^{-1}) in CLDH6-0.5M and CLDH6-1.0M are stronger than those
350 in C0, which is due to the transformation of CLDH to Mg-Al-Cl LDH. The bands near 1424 and
351 859 cm^{-1} indicate that the samples have already absorbed CO_2 molecules from the air before
352 testing. The shoulder at 1091 cm^{-1} comes from the asymmetric stretching vibration of S-O in
353 SO_4^{2-}, which has been designated as the fingerprint peak of AFt in cement paste, analysis of
354 the FT-IR spectra shows that there are no new peaks formed due to the addition of CLDH to
355 the cement and the increase of chloride concentration leads to more formation of AFt.

356

357 In the low-frequency region from 800 to 400 cm^{-1}, four bands near 796, 520, 462, and 416 cm^{-1}
358 are closely related to the formation of Friedel's salt and LDH. For the pure cement paste
359 without Mg-Al CLDH, C0, the bands near 520 and 416 cm^{-1} can be neglected because of the
360 extremely weak strength. The remaining peaks near 796 and 462 cm^{-1} are due to Al-O lattice
361 vibrations of $[Al(OH)_6]^{3-}$, which are fingerprint peaks for Friedel's salt in cement paste. As for
362 the samples with Mg-Al CLDH, CLDH6-0.5M and CLDH6-1.0M, the intensity of the bands
363 near 796, 520, and 416 cm^{-1} are much stronger than compared to C0. The increase in the intensity
364 of the band near 796 cm^{-1} again proves that the use of Mg-Al CLDH in cement pastes promoted
365 the formation Friedel's salt. The bands near 520 and 416 cm^{-1} in Fig.10 should be attributed to
366 Mg-O lattice vibrations in the brucite-like layer. The intensity of the band near 416 cm^{-1}
367 increases with the increase of chloride concentration and this should be a key band for judging
368 the formation of Mg-Al-Cl LDH in cement paste. The stronger intensity of the peak at 416 cm^{-1}
369 confirms that there is more Mg-Al-Cl LDH in CLDH6-1.0M than in CLDH6-0.5M.

370

371 Fig.11 depicts the FT-IR spectra of CLDH6 at different environmental temperatures. When
372 temperature is 20 °C, the corresponding bands near 796, 520, and 416 cm^{-1} are much stronger
373 in intensity, indicating that there is more Friedel's salt and Mg-Al-Cl LDH formed in the
374 sample. When the temperature increases further to 50 °C, there is a significant change in the
375 band near 416 cm^{-1}. The intensity of the band decreased and almost disappeared, which
376 confirms that higher environmental temperature is a disadvantage to the transformation of
377 CLDH to Mg-Al-Cl LDH in cement paste.

378

379 Fig.12 shows the FT-IR spectra of CLDH6-0.5M with the change in pH of the pore solution.
380 As the pH increased, the intensities of the bands near 796, 520, 462, and 416 cm^{-1} gradually
381 decreases, which indicates that the formation of both Friedel's salt and Mg-Al-Cl LDH are
382 impeded due to the increased pore solution alkalinity. When the pH reaches a value of 13.5,
383 the intensities of the bands near 520 and 416 cm^{-1} become very weak, which also indicates that
384 there is little LDH in CLDH6-0.5M-13.5pH. This result is consistent with the XRD and DTG
385 results previously discussed. This result confirms that the formation of Mg-Al-Cl LDH is
386 susceptible to increases in alkalinity.

387 *3.5. Discussions*

3.5.1. Chloride concentration

Even though Mg-Al CLDH has an excellent chloride binding capacity due to memory effects, most of Mg-Al CLDH particles are encased by hydration products of cement in cement paste because the CLDH content is only 6% in these samples. Fig.13(A) shows a schematic representation of these samples. In the initial stages of chloride interaction with the concrete, the total chloride content is low, so the chloride ions will likely be bound by the hydration products of cement paste before coming into contact with CLDH, as shown in Fig.13 (B). In other words, the initial binding of chloride is mainly controlled by the formation of Friedel's salt and the adsorption of C-S-H gel. Then, as the chloride content continues to increase and there is greater penetration into the cement, the uptake of chloride by the cement hydration products around CLDH reaches equilibrium, and more chloride reached the surface of CLDH through capillary pores. Once this critical chloride concentration is reached, CLDH could take part in the adsorption of chloride ions, as shown in Fig.13(C). The excellent anion exchange ability of CLDH then becomes a key factor in determining the chloride binding capacity of cement paste.

3.5.2. Environmental temperature

Both the experimental data and the micro-analyses have demonstrated that higher temperatures will impede the formation of Friedel's salt and Mg-Al-Cl LDH in cement paste. However, the mechanisms affecting the formation of these products are more complicated than those at lower temperatures. Trusilewicz verified the thermal stability of Friedel's salt and found that 35 °C is the temperature at which there is a structural transition between the α-form (monoclinic, < 35 °C) and β-form (rhombohedral, < 35 °C)[26]. Renaudin and Abate *et al.* reported that the dehydration of Friedel's salt started from the structure transition between the α- and β-forms and ended at 28 °C[27, 28]. Therefore, the decomposition of Friedel's salt is an important reason for the decrease in bound chloride content as the temperature exceeded 38 °C in this study. Additionally, the formation of Friedel's salt is closely related to the AFm phase present in the cement (OH-AFm and SO_4^{2-}-AFm)[29]. Glasser and Kindness *et al.* found that SO_4^{2-}-AFm was thermodynamically unstable in the range ~0-40 °C, and only became stable at or above 40 °C[30]. Matschei and Lothenbach *et al.* reported that the stability of OH^-- AFm and SO_4^{2-}-AFm were marginal at 25 °C[23]. DTG analysis showed the absence of AFm phases in CLDH6 when the temperature is 50 °C. However, Glasser *et al.* also thought that SO_4^{2-}-AFm may persist at temperatures around 20 °C, due to the low thermodynamic driving force[30], which is consistent with the DTG results shown in Fi.8. The absence of the AFm phase at 50 °C may be due to the transformation of it to Friedel's salt.

Duan reported that the amount of SO_4^{2-} absorbed by calcined Mg-Al-CO_3 LDH increased as the temperature increased[31]. The explanation for this is the Gibbs-Helmholtz equation, given by: $\Delta G = \Delta H - T\Delta S$, where, ΔG is the change in the system's free energy, ΔH and ΔS are the changes in the system's enthalpy and entropic factors, and T is the temperature of the system. The value of ΔG reflects the driving force of the adsorption process for Mg-Al CLDH. A more negative ΔG value corresponds to a stronger driving force, resulting in easier adsorption. The calculated results reported by Duan showed that the values of ΔG during the adsorption process of Mg-Al CLDH on CO_3^{2-}, SO_4^{2-} and Cl^- were negative. As the temperature increased, ΔG values become increasingly negative, which means that anion adsorption became easier and more anions are absorbed. This is consistent with the bound chloride content change of Mg-Al-Cl LDH from 3 to 38 °C. The reduction in the bound chloride content of Mg-Al-Cl LDH as the temperature reached above 38 °C could be attributed to the competition between CO_3^{2-}, SO_4^{2-}, and Cl^- that entered into the layered structure of the LDH in the cement paste. Although

the concentrations of CO_3^{2-} and SO_4^{2-} are far lower than that of Cl^-, the driving force of adsorption of CO_3^{2-} and SO_4^{2-} is more significant at elevated temperatures. This suggests that CO_3^{2-} and SO_4^{2-} may more easily enter the layered structure compared with Cl^- at the same temperature, which impedes the formation of Mg-Al-Cl LDH. Additionally, higher curing temperatures accelerates the hydration speed of cement, which results in the encasement of CLDH particles by even more hydration products than at lower temperatures. This increases the chloride concentration required to reach the surface of CLDH, as the chloride will first bind to the increased concentration of hydration products, thus impeding the formation of Mg-Al-Cl CLDH.

3.5.3. Pore solution alkalinity

The negative effect of higher alkalinity on the chloride binding of cement paste has been widely reported, which mainly is related to the formation of Friedel's salt being impeded[19][32][33]. It can be explained from the formation and stability of Friedel's salt, respectively. Firstly, there is a competition between OH^- and Cl^- during their adsorption in the interlayers of AFm hydrates of compositon, $[Ca_2Al(OH^-)_6 \cdot nH_2O]^+$, and the former enters the layered structure of AFm prior to the latter. In other words, low pH results in more adsorption sites for free chlorides to form Friedel's salt[34]. Secondly, an increased pH of the chloride solution increases the dissolution of Friedel's salt. Nicolas *et al.* found there was a congruent dissolution process for Friedel's salt with pH value increasing from 10 to 13 (i.e. Ca/Al ratios close to 2 both for solids and solution), and the calculated result shown that the dissolution of Cl from Friedel's salt gradually increased[35].

Higher pore solution alkilinity also leads to the reduciton of chloride adsorption of Mg-Al CLDH. According to the order of the Hofmeister series, OH^- had a stronger exchange ability compared with Cl^-, and it is more stable in LDHs, which meant that OH^- entered the layered structure of LDH prior to Cl^-[36], which is similar to the effect of pore solution alklintiy on the formation of Friedel's salt. Otherwise, at the high pH condition, there are more negative charges on the surface of Mg-Al CLDH due to the adsorption of OH^-, leading to the stronger repulsive interaction between the surface of CLDH and the anions in pore solution. On the other hand, the rehydration of CLDH in cement paste, as shown in Eq. (2), essentially is a chemical adsorption reaction, and OH^- is one of the two reaction products. Increasing pore solution alkalinity increased the concentration of OH^-, and as a result, the rehydration process of CLDH was limited, according to the principle of chemical reaction equilibrium. With an increase of the OH^- concentration in the pore solution, the above negative effects become more significant and lead to reduce Mg-Al-Cl LDH formation.

Beside this, it should be mentioned that there may be a reaction between OH^- and Al^{3+} in the lattices of MgO and $MgAl_2O_4$ of CLDH, leading to the dissolution of Al^{3+} from CLDH and affecting the formation of Mg-Al-Cl LDH. Nevertheless, this need be further confirmed through a serious of experiments.

Absolutely, higher pore solution alkalinity is adverse to both of the formation of Friedel's salt and the rehydration of CLDH. However, CLDH6 still has more bound chlorides compared with C0 at the same pH condition, which can be attributed to the excellent adsorption of CLDH on chloride ions. The data from Shui *et al.* shown Mg-Al CLDH has almost four times the bound chlorides of the blank cement[12].

3.5.4 The effect of CLDH on the formation of Friedel's salt

In terms of Portland cement based materials, the formation process of Friedel's salt can be explained as following reactions:

$$3CaO \cdot Al_2O_3 + 3Ca^{2+} + 3SO_4^{2-} + 6OH^- + 32H_2O \rightarrow \underset{\text{(Ettringite)}}{Ca_6Al_2(SO_4)_3(OH)_{12} \cdot 26H_2O} \quad (6)$$

$$Ca_6Al_2(SO_4)_3(OH)_{12} \cdot 26H_2O + 2(3CaO \cdot Al_2O_3) + 4H_2O \rightarrow \underset{\text{(SO}_4\text{-AFm)}}{3(Ca_4Al_2(SO_4)(OH)_{12} \cdot 6H_2O)} \quad (7)$$

$$Ca_4Al_2(SO_4)(OH)_{12} \cdot 6H_2O + 2Cl^- \rightarrow \underset{\text{(Cl-AFm)}}{Ca_4Al_2(Cl_2)(OH)_{12} \cdot 4H_2O} + SO_4^{2-} + 2H_2O \quad (8)$$

$$3CaO \cdot Al_2O_3 + Ca^{2+} + 2OH^- + 12H_2O \rightarrow Ca_4Al_2(OH)_{13} \cdot 6H_2O \quad (9)$$

$$\text{OH-AFm} + Na^+ + Cl^- \rightarrow \text{Cl-AFm} + Na^+ + OH^- \quad (10)$$

C_3A firstly reacts with gypsum, which is used as cement retarder, to form Ettringite as shown in Eq.(6)[36]. After the depletion of the gypsum in cement, the remainder of C_3A reacts with Ettringite to form monosulfoaluminate (*i.e* SO_4-AFm) as shown in Eq.(7)[36]. When external chloride ions are introduced into cement paste, SO_4-AFm transforms to Friedel's salt (*i.e* Cl-AFm) by anions exchanging between Cl^- and SO_4^{2-} as shown in Eq.(8)[37], and it also should be noted that this anions exchanging reaction need to consume a lot of C_3A because of 1:2 molar ratio of Ettringite to C_3A . Otherwise, Suryavanshi *et al.* thought that if there was still unreacted C_3A in cement paste, it also could react with $Ca(OH)_2$ to form C_4AH_{13}, which was a unstable AFm phase and decomposed to other OH-AFm to form Cl-AFm due to chloride ions displace the OH^- in the interlayers of AFm as illustrated by Eqs. (9) and (10)[29]. In summary, it can be concluded that more C_3A take part in the reaction (7) and (9), the more Friedel' s salt form.

Fig.14 shown the XRD patterns of C0 and CLDH6 before chloride binding test .It can be clearly seen that after 1 day standard curing the peak of Ettringite in CLDH6 is far lower than that in C0 , and the same result also can be found in the XRD patterns of C0 and CLDH6 after 28 days standard curing. Above results demonstrate that the use of Mg-Al CLDH can affect the formation of Etrringite in cement paste, and it initiates from the early stage of hydration (1 day). Mg-Al CLDH has greater adsorption ability of SO_4^{2-}, and form Mg-Al-SO_4 LDH through rehydration which has been explained as shown in Eq.(2). Undoubtedly, this rehydration process on the one hand accelerates the consumption of gypsum and limits the formation of Ettringite, on the other hand, promote more C_3A transforming to Friedel's salt through the reaction (7) and (9). Therefore, the use of Mg-Al CLDH is good for the formation of Friedel's salt in cement paste. Nevertheless, it should be pointed out that the mechanism analyses, explaining the effect of CLDH on the formation of Friedel's salt, are based on the simple chemical reaction equations, and there are still many works should be done , especially about thermodynamics and kinetics studies.

4. Conclusions

A series of experiments on the chloride binding capacity of cement paste with Mg-Al CLDH, with different chloride concentration, environmental temperature, and concrete pore solution alkalinity, is present. It is verified that there is a optimum temperature range for the transformation of Mg-Al CLDH to Mg-Al-Cl LDH in cement paste. Higher pore solution alkalinity is adverse to both of the formation of Friedel's salt and the rehydration of CLDH. The use of Mg-Al CLDH can promote the formation of Friedel's salt in cement paste. Based on the results and analysis, the following conclusions can be drawn:

(1) The improvement of the chloride binding capacity of cement paste with CLDH added is closely related to the initial chloride concentration. XRD, DTG, and FT-IR analysis shows that there is little Mg-Al-Cl LDH formation in cement paste when the chloride concentration is lower. This means that the binding of chloride is mainly controlled by the formation of Friedel's salt and the adsorption of C-S-H gel at low chloride concentrations;

(2) Micro-analysis testing demonstrates that lower and higher environmental temperature is disadvantage to the transformation of Mg-Al CLDH to Mg-Al-Cl LDH in cement paste.The amount of bound chloride at different curing temperatures follows as 38 °C > 50 °C ≈20 °C > 3 °C, and the optimum temperature range for the formation of Mg-Al-Cl LDH in cement paste is from 20 to 38 °C. Besides, using Mg-Al CLDH leads to chloride binding capacity of cement paste becomes more susceptible to the change of environmental temperature;

(3) Higher pore solution alkalinity is adverse to both of the formation of Friedel's salt and the rehydration of CLDH. The improvement of the chloride binding capacity of cement paste with added Mg-Al CLDH become weaker with increasing pH from 12.5 to 13.5, and there is almost no improvement when pH reached 13.5;

(4) Mg-Al CLDH can promote the formation of Friedel's salt. This can be attributed to Mg-Al CLDH promote more C_3A transforming to Friedel's salt through limiting the formation of Ettringite because of the competition between Mg-Al CLDH and C_3A on the adsorption of SO_4^{2-}.

Acknowledgments

This work was fully supported by Natural Science Foundation of Zhejiang Province (No. LY17E080017), Natural Science Foundation of China (No. 51778578), Public welfare foundation of Ningbo city (2019C50015) and Natural Science Foundation of Ningbo City (No. 2019A610392). Authors also thanked Dr Li xie for his help on the XRD patterns analysis.

References

1. Thomas MDA, Hooton RD, Scott A, et al. The effect of supplementary cementitious materials on chloride ions binding in hardened cement paste, Cement Concrete Res. 2012:42: 1-7.

2. Dousti A, Beaudoin JJ, Shekarchi M. Chloride ions binding in hydrated MK, SF and natural zeolite-lime mixtures, Constr Build Mater 2017:154:1035-1047.

3. Talero R, Trusilewicz L, Delgado A, et al. Comparative and semi-quantitative XRD analysis of Friedel's salt originating from pozzolan and Portland cement, Constr Build Mater 2011:25: 2370-2380.

4. Otieno M, Beushausen H, Alexander M. Effect of chemical composition of slag on chloride penetration resistance of concrete, Cement Concrete Comp 2014:46: 56-64.

5. Chakraborty J, Sengupta S, Dasgupta S, et al. Determination of trace level carbonate ion in Mg–Al layered double hydroxide: Its significance on the anion exchange behavior, J. Ind. Eng. Chem 2012:18: 2211-2216.

6. Duan P, Chen W, Ma J, et al. Influence of layered double hydroxides on microstructure and carbonation resistance of sulphoaluminate cement concrete, Constr. Build Mater. 2013:48:601-609.

7. Ke X, Bernal SA, Provis JL. Controlling the reaction kinetics of sodium carbonate-activated slag cements using calcined layered double hydroxides, Cement Concrete Res 2016:81: 24-37.

8. Shui ZH, Yu R, Chen YX, et al. Improvement of concrete carbonation resistance based on a structure modified Layered Double Hydroxides (LDHs): Experiments and mechanism analysis, Constr Build Mater 2018:176: 228-240.

9. Goh KH, Lim T, Dong Z. Application of layered double hydroxides for removal of oxyanions: A review[J]. Water Research 2008:42: 1343-1368.

10. Debecker DP, Gaigneaux EM, Guido B, Exploring, tuning, and exploiting the basicity of hydrotalcites for applications in heterogeneous catalysis, Chemistry 2010:40:3920-3935.

11. Yoon S, Moon J, Bae S, et al. Chloride adsorption by calcined layered double hydroxides in hardened Portland cement paste, Mater. Chem. Phys. 145 (2014) 376-386.

12. Chen Y, Yu R, Wang X, et al. Evaluation and optimization of Ultra-High Performance Concrete (UHPC) subjected to harsh ocean environment: Towards an application of Layered Double Hydroxides (LDHs). Constr Build Mater. 2018:177:51-62.

13. Chen Y, Shui Z, Chen W, et al, Chloride ions binding of synthetic Ca–Al–NO_3 LDHs in hardened cement paste, Constr Build Mater 2015:93:1051-1058.

14. Yang Z, Fischer H, Polder R. Synthesis and characterization of modified hydrotalcites and their ion exchange characteristics in chloride-rich simulated concrete pore solution, Cement Concrete Comp 2014:47: 87-93.

15. Lv L, He J, Wei M, et al. Uptake of chloride ion from aqueous solution by calcined layered double hydroxides: Equilibrium and kinetic studies, Water Res 2006:40: 735-743.

16. Zhang W Y, Liu Y, Xi L J, Adsorption of Chloride Anion by Calcined Mg-Al-Fe Layered Double Hydroxides in Wastewater, Appl. Mech. Materials. 423-426 (2013) 545-549.

17. Yuan Q, Shi CJ, De Schutter G, et al. Chloride ions binding of cement-based materials subjected to external chloride environment-A review, Constr Build Mater 2009:23:1-13.

18. Delagrave A, Marchand J, Ollivier J, et al. Chloride ions binding capacity of various hydrated cement paste systems, Adv. Cem Based Mater 1997:6:28-35.

19. Ipavec A, Vuk T, Gabrovšek R, et al. Chloride ions binding into hydrated blended cements: The influence of limestone and alkalinity, Cement Concrete Res 2013:48:74-85.

20. özgümüş S, Gök MK, Bal A, et al. Study on novel exfoliated polyampholyte nanocomposite hydrogels based on acrylic monomers and Mg–Al–Cl layered double hydroxide: Synthesis and characterization[J]. Chem Eng J 2013:223: 277-286.

21. Yue X, Liu W, Chen Z, et al. Simultaneous removal of Cu(II) and Cr(VI) by Mg–Al–Cl layered double hydroxide and mechanism insight[J]. J Environ Sci 2007:53:16-26.

22. Birnin-Yauri UA, Glasser FP. Friedel's salt, $Ca_2Al(OH)_6(Cl,OH)\cdot 2H_2O$: its solid solutions and their role in chloride ions binding, Cement Concrete Res 1998:28:1713-1723.

23. Matschei T, Lothenbach B, Glasser FP. The AFm phase in Portland cement, Cement Concrete Res 2007:37:118-130.

24. Shi Z, Geiker MR, Lothenbach B, et al. Friedel's salt profiles from thermogravimetric analysis and thermodynamic modelling of Portland cement-based mortars exposed to sodium chloride solution, Cement Concrete Comp 2017:78:73-83.

25. Shaikh FUA, Supit SWM. Chloride induced corrosion durability of high volume fly ash concretes containing nano particles, Constr Build Mater 2015:99:208-225.

26. Trusilewicz LN. Thermal stability of Friedel's salt from metakaolin origin by DSC and HTXRD techniques, J Therm Anal Calorim 2018:134:371-380.

27. Renaudin G, Kubel F, Rivera JP, et al. Structural phase transition and high temperature phase structure of Friedels salt, $3CaO \cdot Al_2O_3 \cdot CaCl_2 \cdot 10H_2O$, Cement Concrete Res 1999:29:1937-1942.

28. Abate C, Scheetz BE. Aqueous Phase Equilibria in the System $CaO\text{-}Al_2O_3\text{-}CaCl_2\text{-}H_2O$: The Significance and Stability of Friedel's Salt, J Am Ceram Soc 2010:78:939-944.

29. Suryavanshi AK, Scantlebury JD, Lyon SB. Mechanism of Friedel's salt formation in cements rich in tri-calcium aluminate, Cement Concrete Res 1996:26:717-727.

30. Glasser FP, Kindness A, Stronach SA. Stability and solubility relationships in AFm phases: Part I. Chloride, sulfate and hydroxide, Cement Concrete Res 1999:29:861-866.

31. Duan P. Research on Modification mechanism and the application of layered double hydroxides for durability of concrete, J. Wuhan Univ Technol 2014.

32. Tritthart J, Pore solution of concrete: The equilibrium of bound and free chloride. Mater Corros 2009:60:579-585.

33. Zhang J, Shi CZ. Zhang ZH. Chloride binding of alkali-activated slag/fly ash cements. Constr Build. Mater 2019:226: 21-31.

34. Mangat PS, Ojedokun OO. Free and bound chloride relationships affecting reinforcement cover in alkali activated concrete. Cement Concrete Comp 2020:112:103692.

35. Marty NCM, Grangeon S, Lerouge C, et al. Dissolution kinetics of hydrated calcium aluminates (AFm-Cl) as a function of pH and at room temperature. Mineral Mag 2017:81:1245-1259.

36. Collins K D, Washabaugh MW. The Hofmeister effect and the behaviour of water at interfaces.Q Rev Biophys, 18(1985) 323-422.

37. Christensen AN, Jensen TR, Hanson JC. Formation of ettringite, $Ca_6Al_2(SO_4)_3(OH)_{12}\cdot 26H_2O$, AFt, and monosulfate, $Ca_4Al_2O_6(SO_4)\cdot 14H_2O$, AFm-14, in hydrothermal hydration of Portland cement and of calcium aluminum oxide-calcium sulfate dihydrate mixtures studied by in situ synchrotron X-ray powder diffraction. J Solid State Chem 2004:177:1944-1951.

38. Weerdt KD, Orsakova D, Geiker MR. The impact of sulphate and magnesium on chloride binding in Portland cement paste, Cem Concr Res 2014:65:30–40.

Table 1. Chemical composition of the cement and LDH used in this study (wt. %).

Materials	SiO_2	CaO	Al_2O_3	Fe_2O_3	MgO	SO_3	K_2O	Loss on ignition
Cement	22.70	57.2	5.09	4.82	3.42	3.27	1.85	1.65
LDH	0.02	0.43	21.8	0.05	77.4	0.23	NA	0.07

Table 2. The mix proportions of different cement pastes used in this study (wt. %).

Mix	Cement	Mg-Al CLDH	W/C
C0	100	-	0.42
CLDH6	94	6	

Table 3. The detailed experimental conditions for the samples in this study.

Group	Samples	Experimental Conditions		
		Content of chloride ions (M)	Curing temperatures (°C)	pH values

A	C0,CLDH6	0.05, 0.25, 0.5, 1, 2, 2.5	20	12.5
B	C0,CLDH6	0.05, 0.5, 1.0	3, 20, 38, 50	12.5
C	C0,CLDH6	0.5	20	12.5, 13.0, 13.5

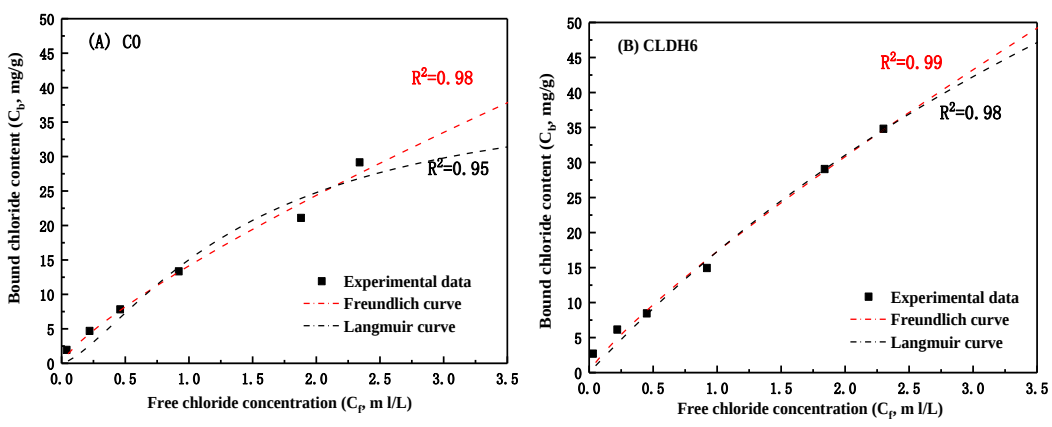

Figure 1. Chloride binding isotherms of C0 (A) and CLDH6 (B) samples at the standard curing

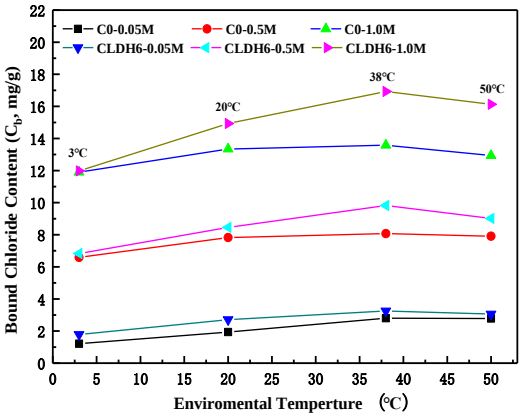

Figure 2. Relationship between Cb, Ci and environmental temperature for C0 and CLDH6 samples.

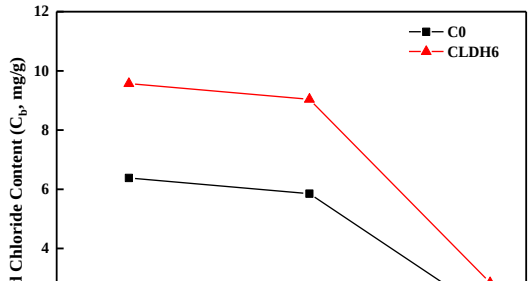

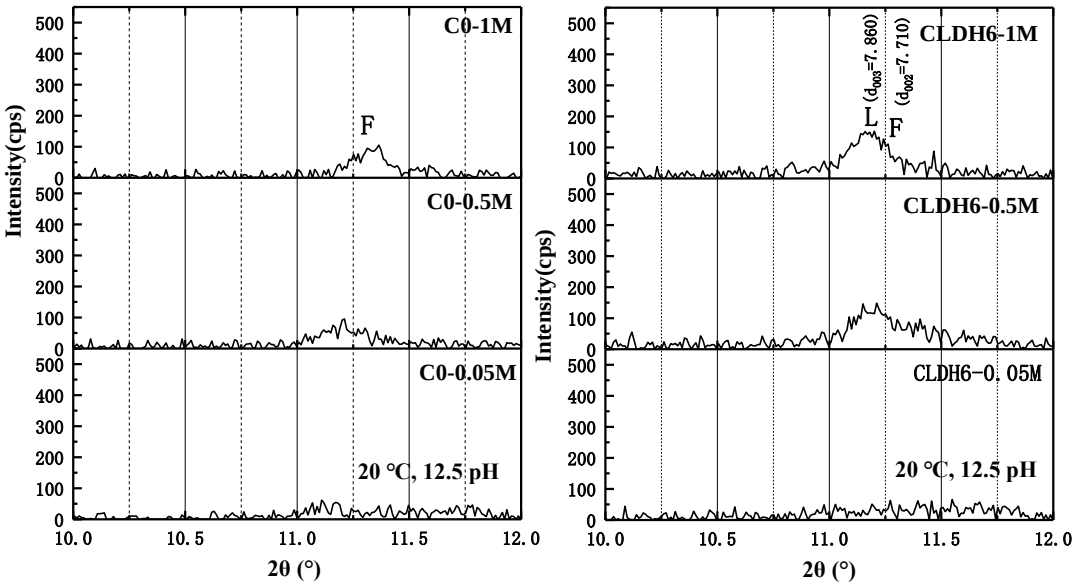

Figure 4. The XRD patterns of C0 (A) and CLDH6 (B) at 20 °C and pH of 12.5, but only including the peaks in the range 2θ = 10° - 12°. (L: Mg-Al Cl LDH, F: Friedel's salt

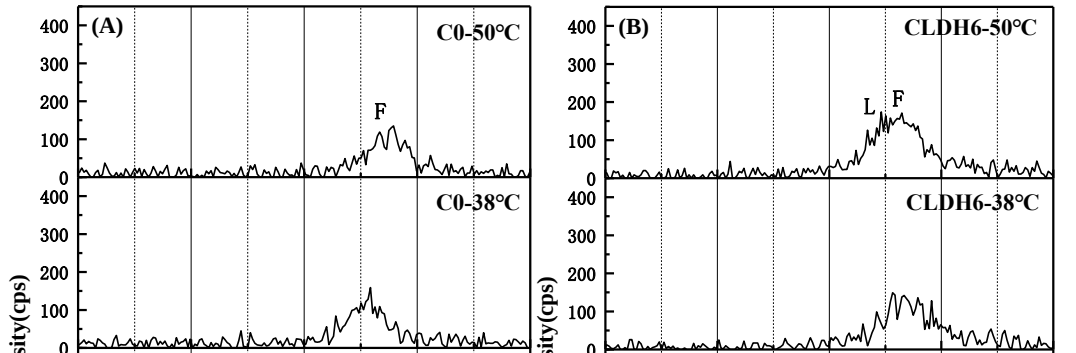

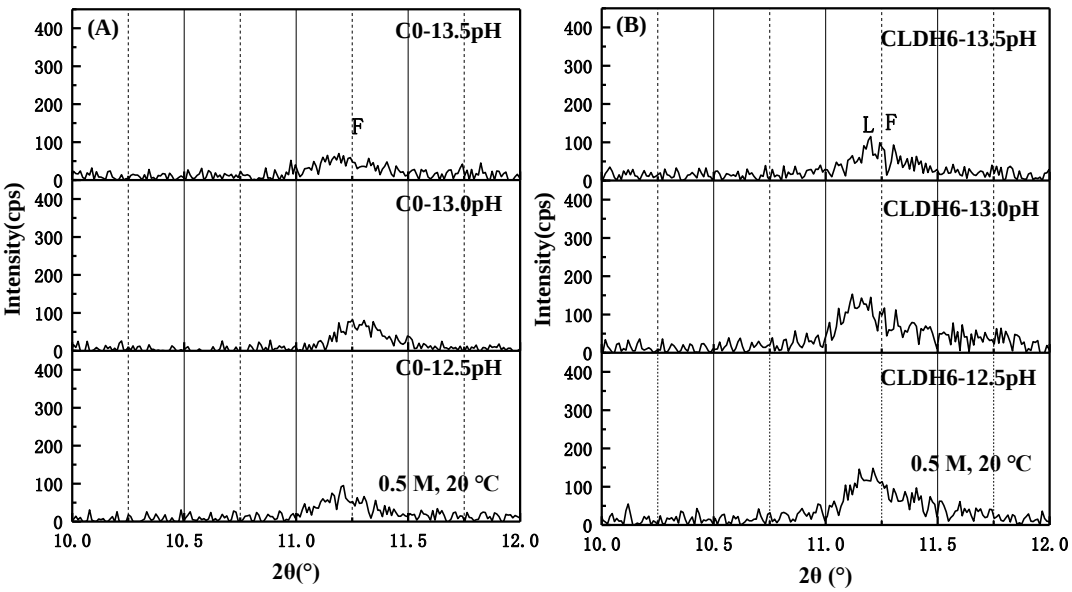

Figure 6. XRD patterns of C0-0.5M (A) and CLDH6-0.5M (B) at 20 °C with initial chloride concentrations of 0.5 M and different pore solution alkalinity conditions.

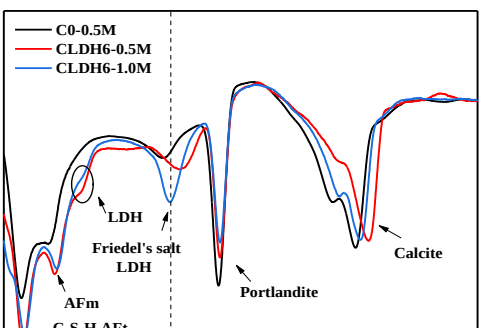

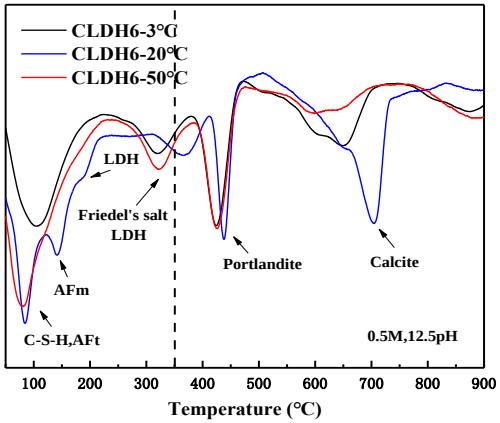

Figure 8. DTG curves of CLDH6-0.5M at pH 12.5 and an initial chloride concentration of 0.5 M at different environmental temperatures.

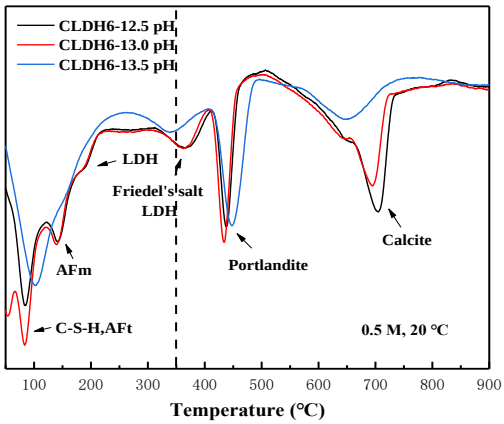

Figure 9. DTG curves of CLDH6-0.5M with different pore solution alkalinities at 20 °C.

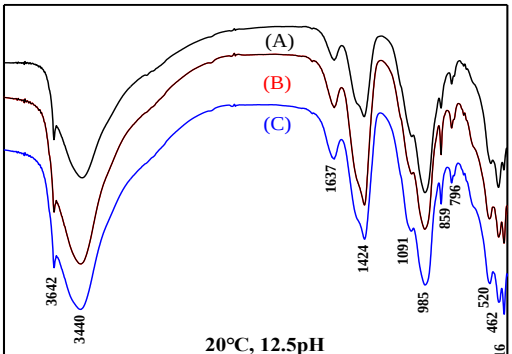

Figure 10. FT-IR spectra of C0 and CLDH6 cured at 20 °C and pH 12.5 with different initial chloride concentrations: (A) C0-0.5M; (B) CLDH6-0.5M; (C) CLDH6-1.0M.

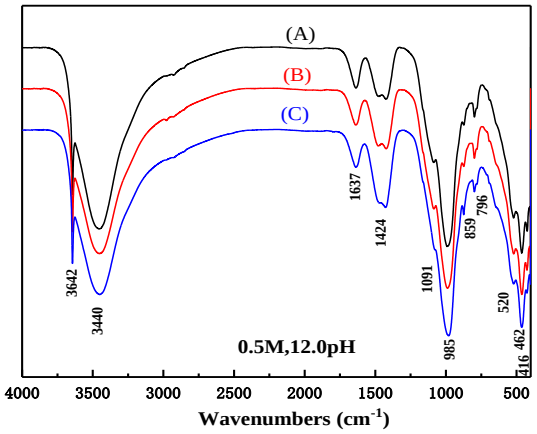

Figure 11. FT-IR spectra of CLDH6 at pH 12 and an initial chloride concentration of 0.5 M at different environmental temperatures: (A) CLDH6-3°C; (B) CLDH6-20°C; (C) CLDH6- 50°C.

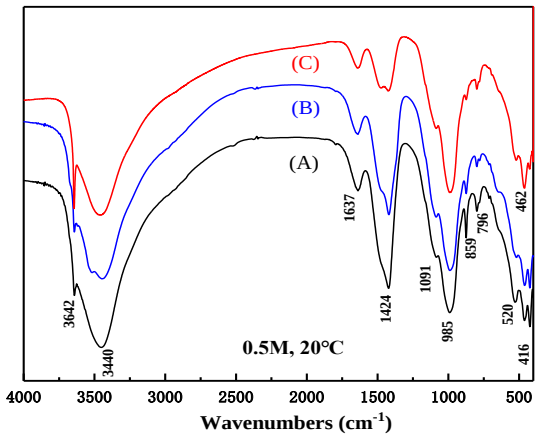

Figure 12. FT-IR spectra of CLDH6-0.5M at 20 °C and an initial chloride concentration. (A) CLDH6-12.5; (B) CLDH6-13.0; (C) CLDH6-13.5.

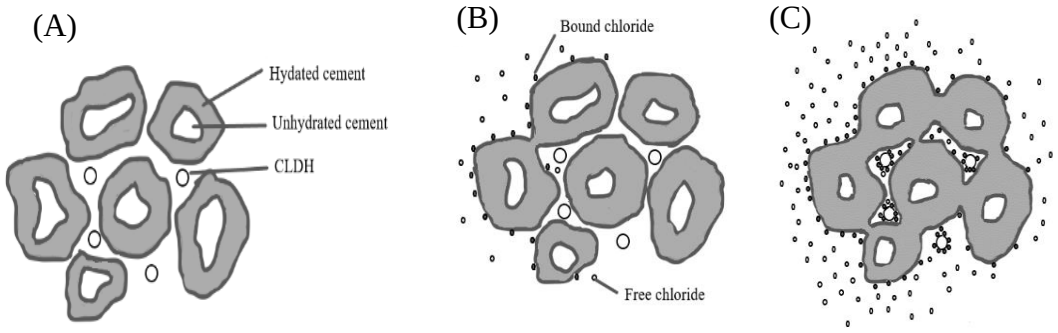

Figure 13. Schematic of chloride binding process in cement paste with CLDH

891

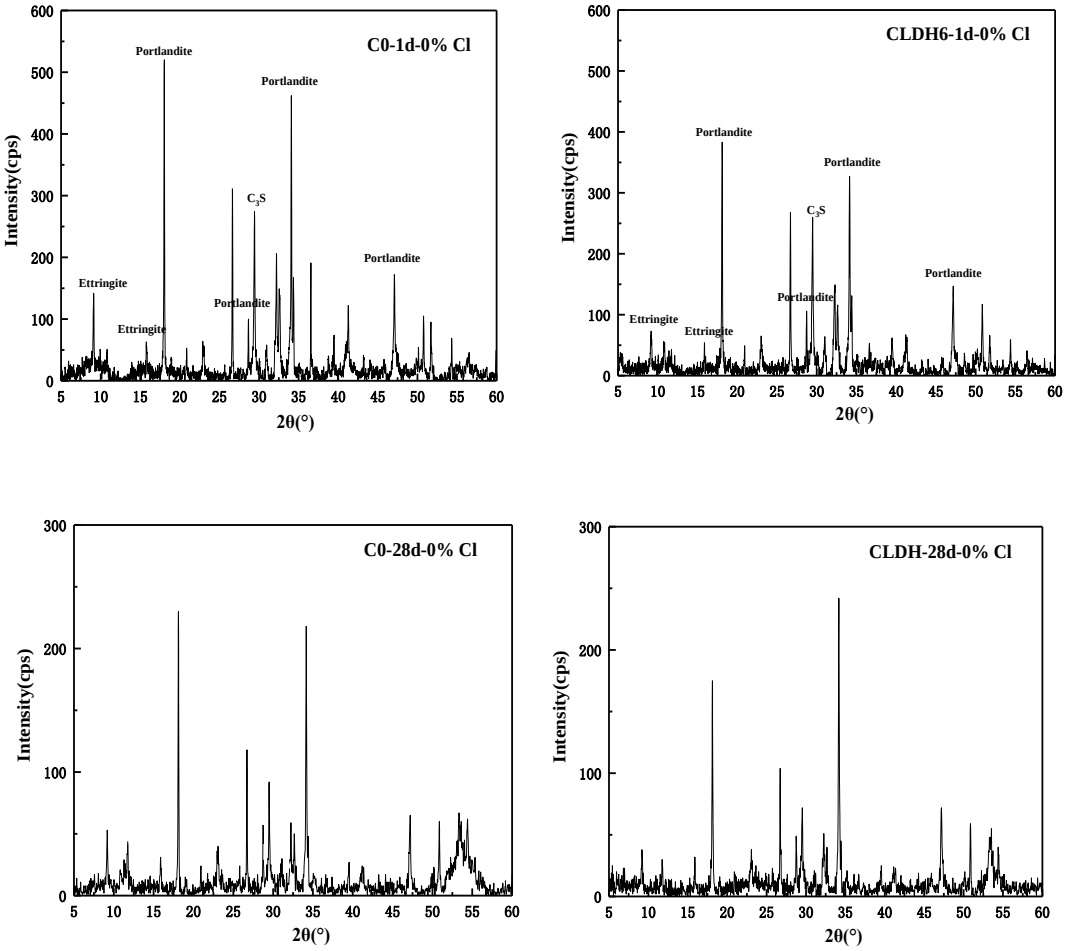

Figure 14. XRD patterns of C0 and CLDH6 after 1 and 28 days standard curing before chloride binding test.

892

893

894

895

896